P6R.4

CONSIDERATIONS FOR COMPARING VOLUMETRIC REFLECTIVITY OBSERVATION BETWEEN SPACE-BORNE AND GROUND-BASED RADARS

Wanyu Li * and V. Chandrasekar
Campus Delivery 1373
Colorado State University, CO, 80523

1. INTRODUCTION

Inter-comparison of reflectivity measurements between the precipitation radar (PR) aboard the Tropical Rainfall Measuring Mission (TRMM) satellite and ground-based validation radars (GR) is made based on the observations for common volumes of precipitation so that the fluctuations in the inter-comparison of the original measurements can be reduced significantly. Several procedures have been developed for the inter-comparison of reflectivities between PR and ground-based radars (Anagnostou et al, 2001, Bolen and Chandrasekar, 2000, 2003, Houze et al, 2004), in order to obtain systematic calibration bias or to compare PR-GR measurement profiles. Bolen and Chandrasekar (2000, 2003) proposed a procedure that can deal with geometric distortion differences between the measurements. Anagnostou et al (2001) and Houze et al (2004) proposed PR-GR relative calibration bias estimation methods using reflectivity data from ice region of the storms or above 0˚C isotherm, which avoid influences of the uncertainties in the data from rain region. The reflectivity bias observation between PR and ground-based radar is one outcome from the inter-comparison of reflectivities for common volumes. The PR-GR bias estimate can have other applications, for example, to calibrate ground radars.

In order to study their contributions to the bias observation, many aspects involving the data acquisition and PR-GR common volume matching should be considered, especially when data from rain region are made use of. Using reflectivity data from rain region, this paper evaluates methods to obtain the bias observation. Coincident data of PR and Kwajalein ground validation radar are used for the evaluation of following effects.

- Effects of difference in PR and GR observation geometries;
- Effects of geometric distortions in PR measurements;
- Effects of differences in radar frequencies;
- Effects of fluctuations in PR attenuation correction.

This paper assumes that the bias observation between PR and GR can be expressed as a simple linear model as follows:

$$b_o = b_{cal} + b_{\delta f} + b_{\delta g} + b_{gd} + b_{pia} + b_{\Delta} \qquad (1)$$

Where b_o is the bias observation from the data; b_{cal} is the differences in the calibrations between the two radar systems; $b_{\delta f}$ is the bias contribution due to the differences in radar frequencies; $b_{\delta g}$ is the bias contribution due to the differences in observation geometries; b_{gd} is the bias contribution due to the geometry distortions in PR's measurements; b_{pia} is the bias contribution due to the fluctuations in PR's reflectivity attenuation correction, and in this paper, this fluctuations are assumed to be caused by the fluctuations in the Path Integrated Attenuation (PIA) measurements; finally, b_{Δ} is the total bias contribution from other factors that are not listed individually. The measurement errors in radar reflectivity factor are considered randomly distributed around zero so they are not taken as a bias contributor.

The paper is organized as follows. The influence of the differences in radar frequencies and its correction is discussed in Section 2. The bias contribution from the fluctuations in PIA is studied in Section 3. Section 4 examines the bias contribution from the differences in radar observation geometries, and the contribution from PR's geometry distortions is studied in Section 5. In the Section 6, the principles of PR-GR reflectivity bias estimation are summarized.

2. COMPARISON OF REFLECTIVITITIES FROM RAIN BETWEEN KU- AND S- BAND

It's well known that for Rayleigh scattering, the reflectivities of different frequencies are the same, and this is the basis that we can obtain the systematic bias estimation through the comparison of reflectivities for

* *Corresponding author address:* Wanyu Li, Colorado State University, Dept. of Electrical and Computer Engineering, Fort Collins, CO. 80523-1373; email: wanyu_li@engr.colostate.edu.

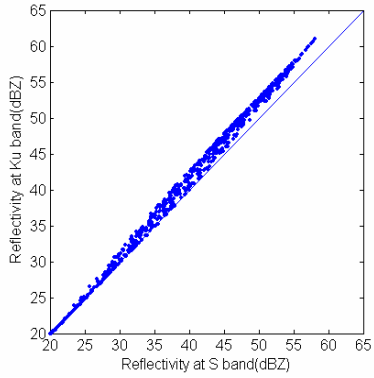

Fig.1. Scatter plot of reflectivities at S-band vs. reflectivities at Ku-band, for widely varying DSD.

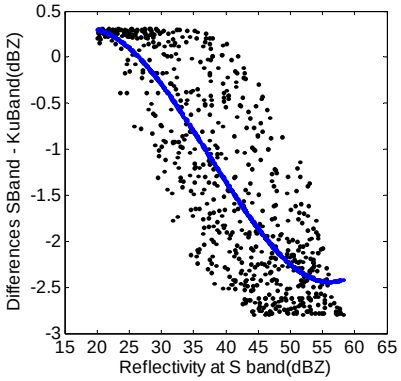

Fig. 2. Scatter Plot of S-band reflectivities vs. differences of reflectivities between S-band and Ku-band. The solid line is the 3-order polynomial fit to the data.

radars being operated at different frequencies. However, due to Mie scattering effect, the reflectivity of high frequencies, like 13.8 GHz at Ku-band for example, for larger sized raindrops is different than the reflectivity of low frequencies at S-band. In practice, to conduct inter-comparison of reflectivities between PR and GR, data around 20 to 30 dBZ are preferred, without consideration of Mie scattering effects. However, in some cases, the data from 20 to 30 dBZ is not enough to make an accurate or reliable estimate and more data of higher value have to be made use of, implying that reflectivities from larger sized raindrops come into the volume. Therefore the differences in reflectivities due to different frequencies should be considered.

The relationship between the reflectivities at the 13.8GHz (Ku band) and 3.0 GHz (S band) for rain can be obtained through scattering computation. Theoretical model of raindrop size distributions are used to study the reflectivity differences. Fig.1 shows the reflectivity at S band vs. reflectivity at Ku band, and Fig. 2 shows

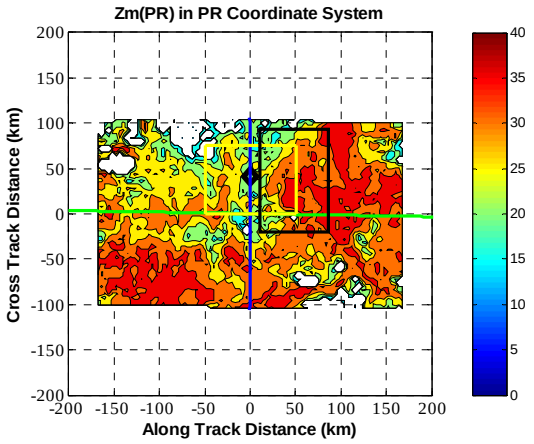

Fig. 3 PR's measured reflectivities at altitude of 2km over Kwajalein radar (diamond) for Jul 02, 2001. Data are from TRMM version 6 product of 2A25. Square in yellow is referred as region 1 and the black square as region 2.

reflectivity at S band vs. the differences of reflectivities between the two frequencies. The scattering computations are conducted for a wide variety of Rain Drop Size Distribution (DSD) parameters (Bolen and Chandrasekar, 2000). In the computation, it is assumed that the S-band radar is horizontally pointing and the Ku-band radar is pointing vertically.

If the formula of $Z_K = Z_S + b$ is used, where Z_K is the reflectivity at Ku-band and Z_S is at S-band, in the regression to the data from 20 to 30 dBZ, the difference (or bias) b between the two frequencies is –0.087 dB, while it is 0.871 dB for data from 30 to 40 dBZ.

In this paper, a 3-order polynomial fit to the data shown in Fig. 2 is used to correct PR reflectivities in order to compare them with GR's. The coincident data of PR and Kwajalein ground validation radar, of Jul 02, 2001, is used to examine the effect of difference in radar frequencies on the bias observation. Fig. 3 shows the measured reflectivities from PR at altitude of 2km. Two regions are chosen to collect data for the study. The scatter plot of PR and GR reflectivities, for region 1 is shown in Fig. 4, and that for region 2 in Fig. 5. The data shown in Fig. 4 and Fig. 5 are for PR-GR matched (common) volumes using the procedure introduced by Bolen and Chandrasekar (2000, 2003). The bias observation between PR and GR is estimated as the offset of the linear fit of the data, with minimum squared error criterion, and it is 2.57dB if data from region 1 are used, and it is 3.24dB when data from region 2 are used. The yellow square in Fig. 3 indicates the location of region 1, while the black square shows region 2. As large as 0.67 dB difference in bias estimate occurs since data from different regions are made use of. Since region 2 contains more intense rain, hence the data of high values contribute more to the bias observation. After PR reflectivities for the common volumes are

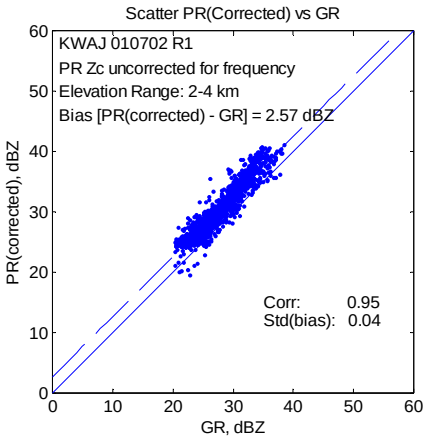

Fig. 4 Scatter plot of reflectivities of PR Vs GR. Data are from region 1, the yellow square as shown in Fig. 3. PR reflectivities are attenuation corrected by TRMM algorithm version 6. Only data larger than 20 dBZ are shown in the plot and used to estimate the bias between the two radars. The bias is 2.57dB.

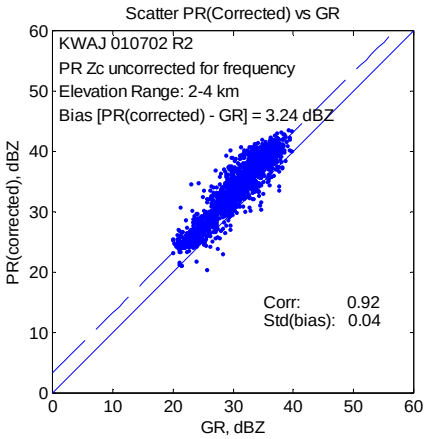

Fig. 5 Scatter plot of reflectivities of PR Vs GR. Data are from the region 2, the black square as shown in Fig. 3. Only data larger than 20 dBZ are shown in the plot and used to estimate the bias between the two radars. The bias is 3.24dB.

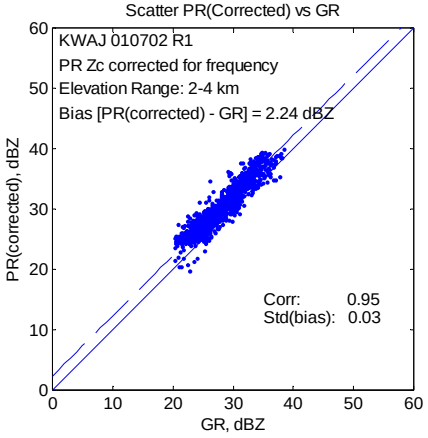

Fig. 6 Scatter plot of PR reflectivities Vs GR reflectivities, for region 1. PR reflectivities are corrected for frequency.

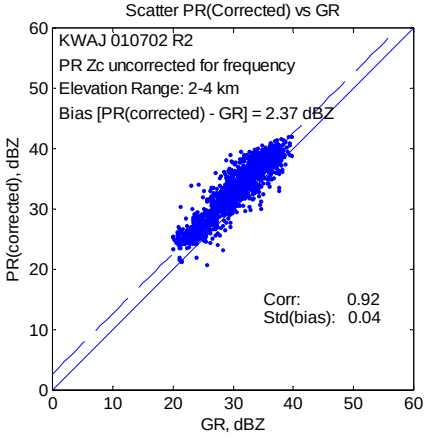

Fig. 7 Scatter plot of PR reflectivities Vs GR reflectivities, for region 2 PR reflectivities are corrected for frequency.

corrected for its frequency, the scatter plots of PR reflectivities Vs GR reflectivities are reproduced and as shown in Fig. 6 and Fig. 7, for the two regions respectively. The bias estimate using data from region 1 then becomes 2.24dB, and it is 2.37dB for area 2. We can see that the estimates become much closer.

3. THE EFFECT OF PR REFLECTIVITY ATTENUATION CORRECTION ON THE BIAS ESTIMATION

TRMM PR is operated at an attenuating frequency, which is 13.8 GHz, and hence it is necessary to make attenuation correction for its reflectivity measurements. TRMM PR basically uses a hybrid of the Hitschfeld-Bordan method and the surface reference method to estimate the vertical profile of attenuation-corrected effective radar reflectivity factor (Z_e) (Iguchi and Meneghini, 1994). The TRMM algorithm estimates the normalized the radar surface cross section (σ_0) first. The two-way PIA is then determined as the decrease of σ_0 compared with its value when there's no rain encountered by the radar beam. The method assumes that the decrease in the surface cross section is caused by the propagation loss in rain. The coefficient α in the k-Z_e relationship $k=\alpha Z_e^{\beta}$ is adjusted in such a way that the PIA will match that estimated from the measured reflectivity profile. This is called α-adjustment method. In order to avoid inaccuracies in the PIA estimation when rain is weak, a hybrid of surface reference method and

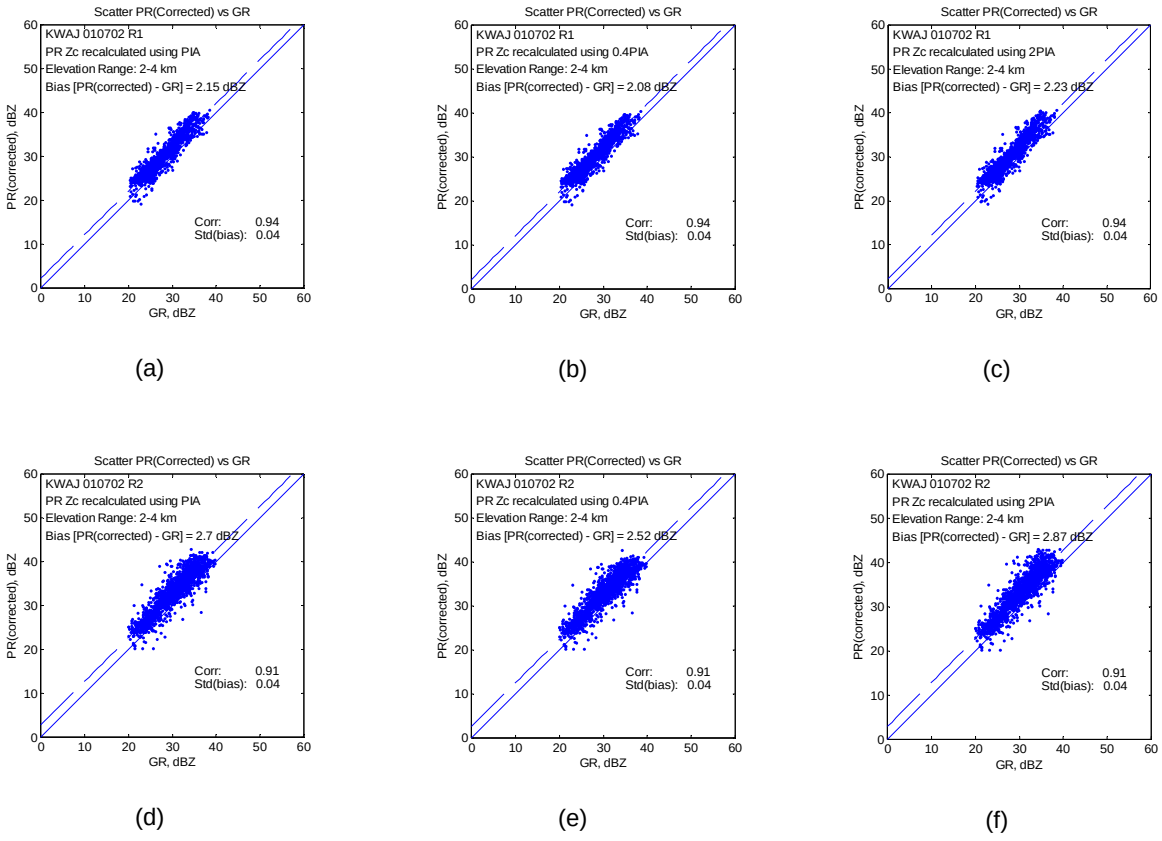

Fig. 8 Scatter plot of PR Z_e Vs. GR reflectivities. PR Z_e are recalculated using hybrid method and PIA from TRMM 2A25 product. (a), (b), and (c) are for region 1, and (d), (e), and (f) for region 2. In (a), and (d), PIA are directly from 2A25 product. In (b), and (e) 40% of the value of PIA given by 2A25 are used. In (c), and (f), 2 times the value of PIA given by 2A25 are used in the calculation.

Hitschfeld-Bordan method is adopted by TRMM (Iguchi and Meneghini, 1994).

Since the fluctuations in PIA estimate is projected directly into the corrected reflectivity (Z_e) through the attenuation correction algorithm, the bias observation between PR and GR, where the Z_e is made use of, could be biased if there's a bias in PIA estimation. The influence of fluctuations in PIA on the PR-GR bias estimation can be evaluated by using recalculated Z_e under assumptions that a certain amount of errors exists in PIA. The attenuation correction procedure of TRMM algorithms actually involves the correction for attenuation caused by cloud liquid water, water vapor and molecular oxygen (TRMM, 2005). In order to make the analysis simple, this paper applies just the hybrid method of Iguchi and Meneghini (1994) to make attenuation corrections.

Over ocean, the standard deviation of normalized radar surface cross section could be from around 2 to 3 dB. (Meneghini et al, 2000), or say the relative errors from 50% to 100%, with the errors around the nadir being smaller. The accuracy of PIA estimate also relies on the accuracy of PR reflectivity measurements. Since PR reflectivity accuracy is 1 dB (3σ error) (Kozu, 2001), the error in PIA is at least this much. To simulate the errors in PIA, this paper uses -60% and 100% as the fluctuation limits for PIA. PR Z_e profiles of the data set of Jul 02, 2001 are recalculated using PIA with -60%, 0% and 100% errors. Fig. 8 shows scatter plot of reflectivities of GR vs. PR Z_e that are recalculated using the hybrid method and PIA data from TRMM 2A25 product. As we can see that, for the data from region 1, the bias contribution from the errors in PIA is -0.07 and 0.08 dB, for PIA's relative error being -60% and 100% respectively, while for region 2, it is -0.18 and 0.17 dB, respectively.

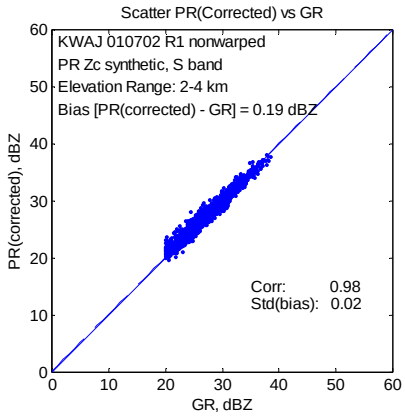

Fig. 9 Scatter plot of synthetic PR reflectivities Vs. GR reflectivities, for region 1.

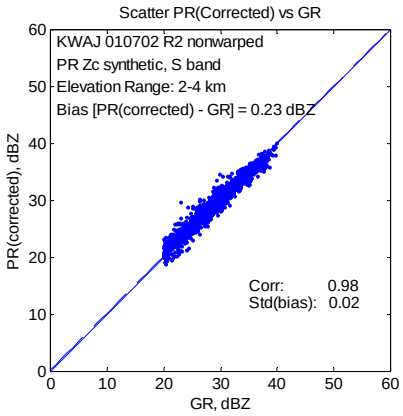

Fig. 10 Scatter plot of synthetic PR reflectivities Vs. GR reflectivities, for region 2.

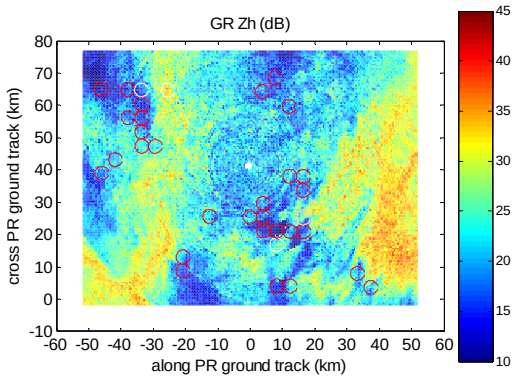

Fig. 11 GR reflectivities at altitude of 2km above the ground. Red circles indicate where PR Zc- GR Zh > 2.5 dB, while white ones for PR Zc – GR Zh < -2.5 dB. Note that the image is just for altitude of 2km, but the circles are for all points in the vertical profiles that match the conditions.

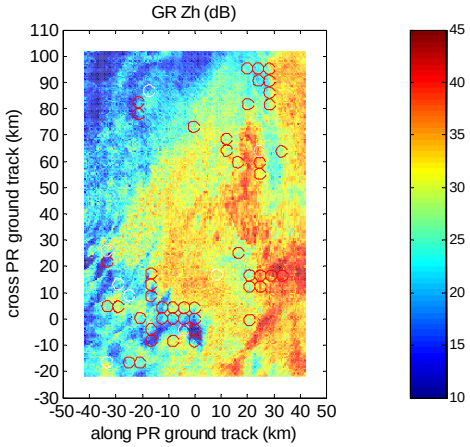

Fig. 12 Similar to Fig. 11 but for region 2.

Region 2 contains more intense rain area, and more attenuation is expected. Hence the fluctuations in PIA have more influence onto the reflectivity bias estimation between the PR and GR.

Although the fluctuation in PR-GR bias observation caused by the fluctuations in PIA may be different than that when actual TRMM attenuation correction algorithms are used, however the method can be applied to TRMM attenuation correction algorithms.

4. THE EFFECT OF DIFFERENCE IN OBSERVATION GEOMETRIES ON THE BIAS ESTIMATION

Due to the differences in the system characterizations and observing geometries, the reflectivity observations are not from common volumes. This paper assumes that each of the radars has pencil beam pattern with width equal to its 3-dB beam width, and range resolution is determined by radar pulse width. The common volume is defined as a cubic area centered on the center of the PR's resolution volume with horizontal extents taken as the maximum horizontal extents from the resolution volumes of the two radars for that central point, and the vertical extent as the maximum vertical extents from the resolution volumes of the two radars. The actual sizes of common volumes may vary from place to place. To obtain reflectivity measurements for the common volumes, the original measurements of the

Table I The bias estimation and contributions from the factors, for the studied regions of the case of Jul 02, 2001.

	b_o	$b_{\delta f}$	b_{pia}	$b_{\delta g}$	b_{gd}
Region 1	2.57	0.33	-0.07~0.08	0.19	-0.15
Region 2	3.24	0.87	-0.18~0.17	0.23	0.13

two radars are re-sampled, and data on Cartesian grids spaced 0.5km by 0.5 km horizontally, and 0.25km vertically are obtained. The reflectivity for a common volume is the average of the reflectivities for the grid points included in the cubic common volume. The difference in the reflectivities for the common volume between the two radars is then calculated and the bias observation is made as the mean of the reflectivity differences over all common volumes. This method actually is made use of throughout the paper. For the case of Jul 02, 2001, a synthetic PR reflectivity data set is obtained from GR data, assuming that there's not Mie scattering effect. In the synthesis of PR reflectivities, the reflectivity for PR resolution volume is obtained through averaging the GR reflectivities on the grids included in the PR resolution volume. Then the PR reflectivities for the common volumes are obtained using the method discussed earlier in this section. The bias observation based on this simulation of PR measurements is then conducted, and the scatter plots of reflectivities of PR Vs GR are shown in Fig. 9 and Fig. 10, for the two regions respectively.

We can see from the scatter plots that the difference in radar observation geometries and the matching procedure contribute bias in the inter-comparison. This is effective especially when rain intensity is non-homogeneous. From Fig. 10 and Fig. 11, it can be seen that large differences in the inter-comparison happen at the edges of the storms where rain intensity varies severely. Compared to the bias caused by the fluctuations in PIA, this part of bias contribution is larger, and should be estimated and considered in order to obtain an accurate PR-GR systematic bias estimation.

5. THE EFFECT OF GEOMETRIC DISTORTIONS IN PR'S MEASUREMENTS ON THE BIAS ESTIMATION

Due to the stability limits in the satellite movements, PR's measurements of the storm are subject to geometric distortions. Bolen and Chandrasekar (2000, 2003) discussed the effects of the perturbations in PR's statures, such as yaw, pitch and roll angles. Of course, if the precipitation is homogeneous within the region chosen to conduct inter-comparison, the movement perturbations will not have any influences onto the measurements.

In this section, we conduct simulations on the effects of PR's movement perturbations using GR reflectivity data from the regions we have studied for. We assume that the perturbations in the three PR's stature angles are stable during PR's observation throughout the regions. The method to obtain PR's synthetic reflectivities for common volumes is the same as that discussed in Section 4, except that the locations of PR's resolution volumes are perturbed. It should be noted that the simulation results are influenced by the effects of both differences in observation geometries and the PR's movement perturbations. Scatter plots of the synthetic PR's reflectivities with a certain geometric distortion Vs GR's reflectivities are shown in Fig. 13. Compared with the bias estimate results when there's not any of the perturbations, as shown in Fig. 9 and Fig. 10, we can see that the perturbations in PR's observation geometry can bring in an extra bias, which is -0.15dB, the maximum for region 1 and 0.13dB, the maximum for region 2.

6. SUMMARY

Inter-comparison of reflectivities between space-born PR and ground based radars can be a very challenging task. Many aspects should be observed in order to obtain an accurate systematic bias observation between PR and GR. This paper discussed the contributions, to the final bias estimate, of four effects, namely, the differences in radar operating frequencies, the differences in radar observation geometries, PR's geometric distortions, and fluctuations in PR's reflectivity attenuation correction. The bias contributions of these factors observed from a coincident data set of PR and Kwajalein radar on Jul 02, 2001 are listed in Table I. We can see that the differences in the radar frequencies could be the major contributor to the final bias estimate, while other factors are equally significant. This observation was confirmed by the study over several other data sets collected by PR and GR over Kwajalein.

Assuming that $b_{\Delta} = 0$, Eq. (1) can be used to estimate the difference in PR and GR calibrations. From Eq. (1), it follows that

$$b_{cal} = b_o - b_{\delta f} - b_{\delta g} + \Delta \qquad (2)$$

Where Δ is the uncertainty term contributed by the effects of PR's geometric distortions and the fluctuations

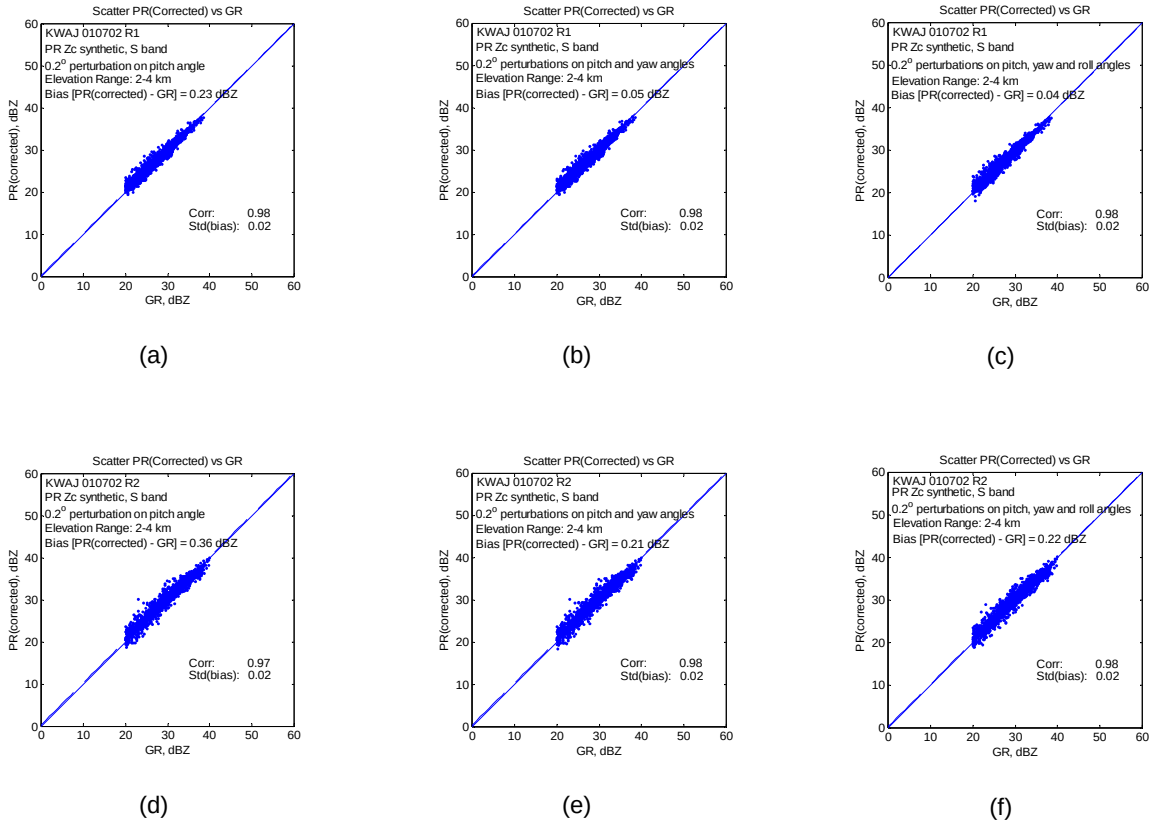

Fig. 13 Scatter plots of synthetic PR reflectivities Vs GR reflectivities. PR is assumed to be at S band. (a), (b), and (c) are for region 1, and (d), (e), and (f) are for region 2. In (a) and (d), a perturbation of 0.2 degrees is applied onto PR's pitch angle. In (b) and (e), perturbations of 0.2 degrees are applied onto PR's pitch and yaw angles. In (c) and (f), each of the three angles has a 0.2 degrees perturbation.

in PIA. Since the value of $b_{\delta g}$ and $b_{\delta r}$ in Eq. (1) can be considered fixed for certain regions from where data are collected, they can be extracted from b_o to evaluate the calibration difference between PR and GR. The boundaries of Δ can be estimated by assuming that effects of fluctuations in PIA and PR's geometry distortions are in the worst situations. Therefore, for the two regions of the data, the calibration differences are:

2.15 dB with error within -0.22 ~0.12 dB for region 1;

2.14 dB with error within -0.19~0.30 dB for region 2.

The calibration difference between PR and Kwajalein radar, from this data set, can be evaluated to be 2.145dB with error within -0.22~0.30dB.

In summary, the principles to conduct PR-GR systematic reflectivity bias estimation can be concluded as follows:

1. For a given PR-GR coincident data set, choose the region with reflectivities between 20 ~ 30 dBZ and choose it as large as possible to include more data;
2. The effect of differences in radar frequencies should be considered if reflectivity data with high values are included in the inter-comparison. This paper gives an example on how to make the corrections on PR's data for this effect. An accurate correction requires the distributions of the DSD parameters for the location where the inter-comparison is made for;
3. The effect of differences in radar observation geometries and common volume matching should be examined and the total effect could be eliminated since for a certain inter-comparison, this effect is certain;
4. The effect of fluctuations in PIA need be considered. Since this part of effects is uncertain and relies on the attenuation correction algorithm, one only could know the ranges of the uncertainty by applying exact algorithms which are used by TRMM PR;

5. The effect of the geometric distortions could be comparable to that caused by fluctuations in PIA or by the difference in radar observation geometries. Its contribution ranges to the systematic bias estimate can be evaluated under all possible perturbation combinations in PR's stature angles and its height.

ACKNOWLEDGEMENTS

This work was supported by the NASA Tropical Rainfall Measuring Mission (TRMM) Program.

REFERENCES

Anagnostou, E., C. Morales, and T. Dinku, 2001: The use of TRMM precipitation radar observations in determining ground radar calibration biases. *J. Atmos. Oceanic Technol.*,**18**, 616-628.

Bolen S. M. and V. Chandrasekar, 2000, Quantitative cross validation of space-based radar observations. *J. Appl. Meteor*., **39**, 2071-2079.

--, and V. Chandrasekar, 2003, Methodology for aligning and comparing spaceborne radar and ground-based radar observations. *J. Atmos. Oceanic Technol.*, **20**, 647-659.

Houze R. A. Jr., S. Brodzik, C. Schumacher, and S. E. Yuter, 2004, Uncertainties in oceanic radar rain maps at Kwajalein and implications for satellite validation. *J. Appl. Meteor*., **43**, 1114-1132.

Iguchi T, and R. Meneghini, 1994, Intercomparison of single-frequency methods for retrieving a vertical rain profile from airborne or spaceborne radar data. *J. Atmos. Oceanic Technol.*, **11**, 1507-1516.

Kozu T, T. Kawanishi, H. Kuroiwa, M. Kojima, K. Oikawa, H. Kumagai, K. Okamoto, M. Okumura, H. Nakatsuka, and K. Nishikawa, 2001, Development of precipitatin radar onboard the Tropical Rainfall Measuring Mission(TRMM) satellite. *IEEE Trans. Geoscience and Remote Sensing*, 39, 102-116.

Meneghini R., T. Iguchi, T. Kozu, L. Liao, K. Okamoto, J. A. Jones, and J. Kwiatkowski, 2000, Use of the surface reference technique for path attenuation estimates from the TRMM precipitation radar. *J. Appl. Meteor*., **39**, 2053-2070.

--, J. A. Jones, T. Iguchi, K. Okamoto, and J. Kwiatkowski, 2004, A hybrid surface reference technique and its application to the TRMM precipitation radar. *J. Atmos. Oceanic Technol.*, **21**, 1645-1658.